Table S1. The effect of substrate particle size (*d*) and moisture (*W*) on the mean tunnel depth ($\bar{D}$ ± s.d.) and mean tunnel volume ($\bar{V}$ ± s.d.).

W	*d, mm*	$\bar{D} \pm s.d., cm$	$\bar{V} \pm s.d., cm^3$
0.01	0.025	3.2 ± 0.9	0.5 ± 0.3
0.03	0.025	3.6 ± 3.5	0.6 ± 0.4
0.05	0.025	6.9 ± 5	1.1 ± 0.3
0.1	0.025	9 ± 3.9	1.6 ± 0.6
0.15	0.025	9.4 ± 3.9	1.4 ± 0.7
0.18	0.025	9.9 ± 2.5	1.8 ± 1
0.2	0.025	7.8 ±2.5	1.4 ± 0.5

W	*d, mm*	$\bar{D} \pm s.d., cm$	$\bar{V} \pm s.d., cm^3$
0.01	0.24	4.4 ± 2.4	0.4 ± 0.3
0.03	0.24	8.1 ± 3.6	0.9 ± 0.7
0.05	0.24	11.6 ± 1.8	1.9 ± 0.6
0.1	0.24	10.1 ± 3.1	1.3 ± 0.8
0.15	0.24	12.5 ± 1.5	1.9 ± 0.7
0.18	0.24	9.3 ± 2.5	1 ± 0.7
0.2	0.24	12.2 ± 1.7	1.7 ± 0.9

W	*d, mm*	$\bar{D} \pm s.d., cm$	$\bar{V} \pm s.d., cm^3$
0.01	0.7	5.1 ± 4.2	1.1 ± 0.5
0.03	0.7	7.2 ± 4.2	1.1 ± 0.7
0.05	0.7	7.4 ± 4.9	1.3 ±1
0.1	0.7	9.6 ± 3	1.5 ± 0.6
0.15	0.7	8.4 ± 2.9	1.4 ± 0.5
0.18	0.7	5.8 ± 3.7	1.3 ± 0.7
0.2	0.7	4.3 ± 3.1	1.1 ± 0.5

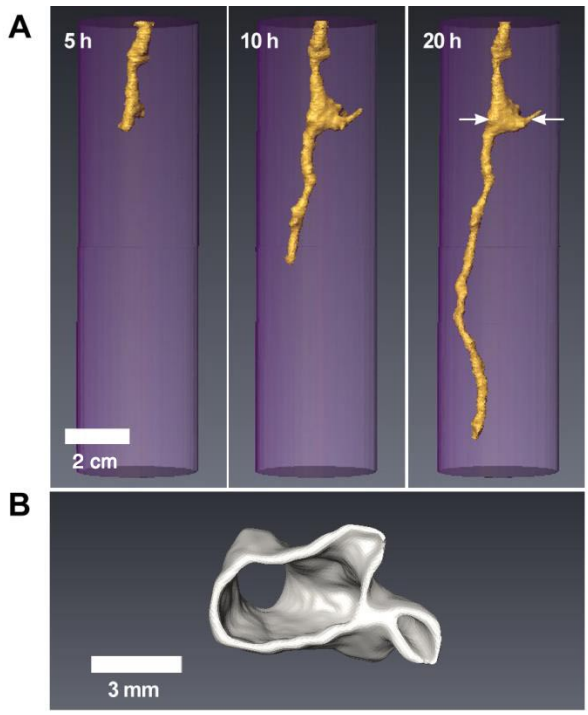

Fig. S1. Example of 3D chambers. A) Time lapse of construction of the tunnel with 3D chamber. Arrows show the height at which the chamber cross-section B) was taken.

Table S2. The effect of substrate particle size (d) and moisture (W) on the mean pellet size ($\bar{A}_p \pm$ s.d.) and maximum pellet size (A_{max}) created by small and large ants of head-size (h).

d (mm)	W	h (mm)	$\bar{A}_p \pm$ s.d. (mm^2)	$A_{max} \pm$ s.d. (mm^2)
0.025	0.01	0.7	0.38 ± 0.21	1.65
		1.2	0.49 ± 0.29	1.32
	0.1	0.7	0.49 ± 0.34	1.66
		1.2	0.49 ± 0.35	2.86
0.24	0.01	0.7	0.27 ± 0.17	1.1
		1.2	0.48 ± 0.31	1.74
	0.1	0.7	0.28 ± 0.15	1
		1.2	0.56 ± 0.3	1.64
0.7	0.01	0.7	0.38 ± 0.19	1.85
		1.2	0.38 ± 0.15	1.1
	0.1	0.7	0.42 ± 0.18	1.32
		1.2	0.42 ± 0.21	1.21

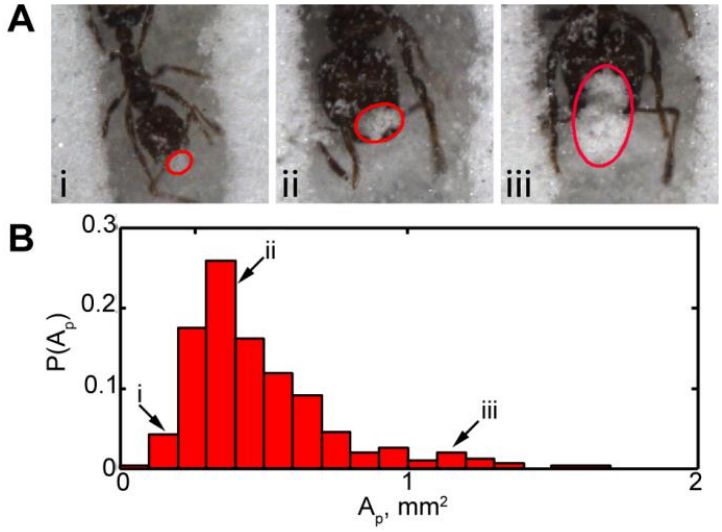

Fig. S2. Distribution of pellet sizes excavated in experiment. A) Examples of pellets created by *S. invicta* in d = 0.025 mm substrate, B). Labels i,ii,iii show snapshots of ants carrying representative pellets from the indicated points in the distribution B). The red ellipses enclose the pellet and are drawn to guide the eye.

Table S3. Estimates of capillary forces, ant strength and particle weight.

d (mm)	Capillary force (μN)	Single particle weight (μN)
0.025	5. 65	0.0002
0.24	54.26	0.18
0.7	158.26	4.4
Ant pulling force (μN)	1256	

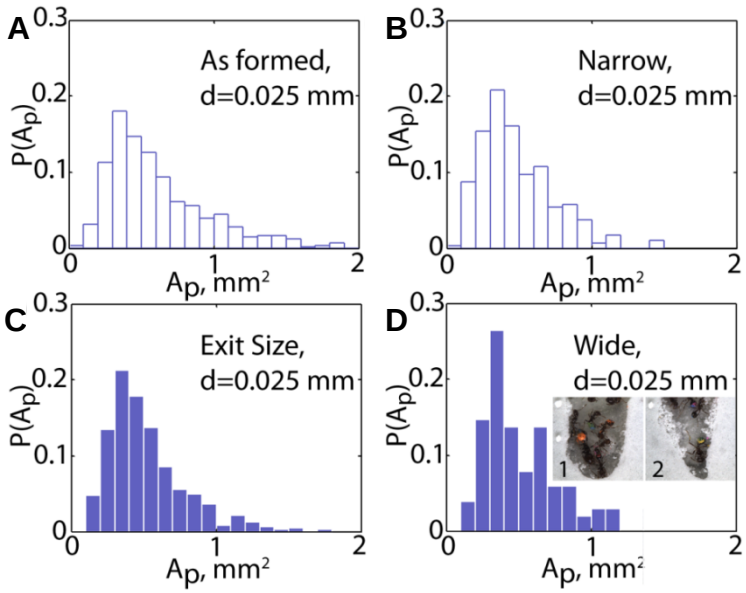

Fig. S3. Pellet size distribution in d = 0.025 mm substrate directly after pellet formation (A) and 3-4 B.L. away from the tunnel face (referred to as 'Exit size') (C). Probability distribution of pellet area carried *by S. invicta* in case of narrow (B) (≤ 0.5 cm) and wide (~1 cm) (d) incipient tunnels in 0.025 mm substrate, W = 0.1. Insert: Tunnel narrowing by ants with time.

Movie 1. "Pulling mode": Typical excavation behavior of *S. invicta* worker (recorded at 50 fps, playing at 30 fps).

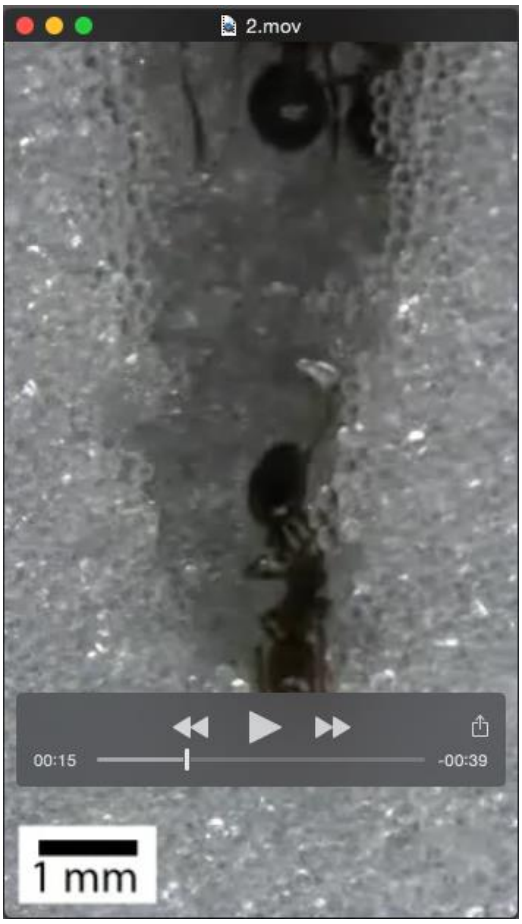

Movie 2. "Formation mode": Typical excavation behavior of *S. invicta* worker (recorded at 50 fps, playing at 20 fps).

Movie 3. Example of pellet breakage due to the ants contact in the tunnel (recorded at 50 fps, playing at 30 fps).

Movie 4. Unsteady locomotion of the *S. invicta* worker, carrying relatively large pellet (recorded at 50 fps, playing at 15 fps).